JOURNAL OF GEOPHYSICAL RESEARCH, VOL. 113, D10211, doi:10.1029/2007JD009624, 2008

Click Here for Full Article

Variations of tropical upper tropospheric clouds with sea surface temperature and implications for radiative effects

Hui Su,[1] Jonathan H. Jiang,[1] Yu Gu,[2] J. David Neelin,[2] Brian H. Kahn,[1] Daniel Feldman,[3] Yuk L. Yung,[3] Joe W. Waters,[1] Nathaniel J. Livesey,[1] Michelle L. Santee,[1] and William G. Read[1]

Received 19 November 2007; revised 18 January 2008; accepted 18 February 2008; published 31 May 2008.

[1] The variations of tropical upper tropospheric (UT) clouds with sea surface temperature (SST) are analyzed using effective cloud fraction from the Atmospheric Infrared Sounder (AIRS) on Aqua and ice water content (IWC) from the Microwave Limb Sounder (MLS) on Aura. The analyses are limited to UT clouds above 300 hPa. Our analyses do not suggest a negative correlation of tropical-mean UT cloud fraction with the cloud-weighted SST (CWT). Instead, both tropical-mean UT cloud fraction and IWC are found to increase with CWT, although their correlations with CWT are rather weak. The rate of increase of UT cloud fraction with CWT is comparable to that of precipitation, while the UT IWC and ice water path (IWP) increase more strongly with CWT. The radiative effect of UT clouds is investigated, and they are shown to provide a net warming at the top of the atmosphere. An increase of IWP with SST yields an increase of net warming that corresponds to a positive feedback, until the UT IWP exceeds a value about 50% greater than presently observed by MLS. Further increases of the UT IWP would favor the shortwave cooling effect, causing a negative feedback. Sensitivities of UT cloud forcing to the uncertainties in UT CFR and IWC measurements are discussed.

Citation: Su, H., et al. (2008), Variations of tropical upper tropospheric clouds with sea surface temperature and implications for radiative effects, *J. Geophys. Res.*, *113*, D10211, doi:10.1029/2007JD009624.

1. Introduction

[2] High-altitude clouds have important radiative effects on the Earth-atmosphere system. They are closely related to upper tropospheric humidity (UTH), which is the dominant contributor to the greenhouse effect [e.g., *Betts*, 1990; *Lindzen*, 1990; *Sun and Lindzen*, 1993; *Udelhofen and Hartmann*, 1995; *Soden and Fu*, 1995; *Su et al.*, 2006a]. They also provide significant radiative forcing to the climate system in their own right. Their net radiative effect results from a balance between warming from reduction of terrestrial emission to space and cooling by reflection of incoming solar radiation. Quantification of the net effect is subject to errors in both longwave (LW) and shortwave (SW) radiative flux measurements, or in model calculations. The net radiative effect of high-level clouds depends on cloud height, optical thickness, areal fraction and cloud microphysical properties such as ice particle size and ice habits. Accurate representation of clouds, their radiative effects and associated climate feedbacks is one of the greatest challenges in climate model simulations and climate change predictions [*Cess et al.*, 1990, 1996; *Stephens*, 2005].

[3] High-altitude clouds in the tropics include deep convective towers and associated anvil clouds, as well as thin cirrus that can be formed in situ by gravity wave and Kelvin wave perturbations or by large-scale uplift of humid layers [*Massie et al.*, 2002]. The relationships of deep convection and associated clouds to sea surface temperature (SST) are of great interest in climate studies because of their importance for cumulus parameterizations in models and their potential implications for cloud feedbacks in climate change. A number of studies have been conducted using various measures of cloud observations and numerical models [e.g., *Graham and Barnett*, 1987; *Waliser et al.*, 1993; *Ramanathan and Collins*, 1991, hereafter RC1991; *Lau et al.*, 1997; *Tompkins and Craig*, 1999; *Lindzen et al.*, 2001, hereafter LCH2001; *Hartmann and Larson*, 2002; *Del Genio and Kovari*, 2002; *Bony et al.*, 2004; *Lin et al.*, 2006]. However, no consensus has been reached regarding whether high-altitude clouds increase or decrease with SST and whether they provide a positive or negative climate feedback. For example, RC1991 showed that the radiative forcing of cirrus anvils increases during El Niño; and the increase of their SW cooling effect is larger than the increase of their LW warming effect. They suggested that the optical thickness of cirrus anvils must increase when SST increases, in addition to the increase in the extent of cloudiness and the height of cloud top. They speculated that

[1]Jet Propulsion Laboratory, California Institute of Technology, Pasadena, California, USA.
[2]Department of Atmospheric and Oceanic Sciences, University of California, Los Angeles, California, USA.
[3]Division of Geological and Planetary Sciences, California Institute of Technology, Pasadena, California, USA.

Copyright 2008 by the American Geophysical Union.
0148-0227/08/2007JD009624$09.00

cirrus anvils may act like a "thermostat" to limit further warming of SST. This viewpoint has been challenged by a number of studies that highlighted the roles of evaporation, large-scale circulation, and ocean dynamics in regulating tropical SST [*Wallace*, 1992; *Fu et al.*, 1992; *Hartmann and Michelsen*, 1993; *Pierrehumbert*, 1995; *Sun and Liu*, 1996].

[4] Another viewpoint regarding the cirrus-SST relation and its climate feedback is the "iris hypothesis" proposed in LCH2001, in which cirrus anvil coverage averaged over the western Pacific was found to decrease with the cloud-weighted SST (CWT, defined as the average SST weighted by cloud fraction for the area 130°E–170°W, 30°S–30°N). The cloud data were based on the infrared brightness temperature (T_b of 11 and 12 μm wavelengths) from the Japanese Geostationary Meteorological Satellite (GMS). In order to account for the impact of changing large-scale circulation and SST gradients on clouds [*Lindzen and Nigam*, 1987; *Hartmann and Michelsen*, 1993; *Lau et al.*, 1997; *Bony et al.*, 2004], LCH2001 postulated a normalization procedure in which cirrus anvil coverage was divided by the cumulus coverage. It attempted to deal with the varying detrainment from cumulus convection when SST changes rather than varying cumulus convection itself, which may be related to shifting patterns of large-scale circulation and SST gradients. Such an attempt is reasonable but the normalization would work only if cirrus anvil coverage were proportional to the cumulus coverage. Without addressing the pre-conditions for the normalization procedure, LCH2001 claimed that cirrus coverage normalized by cumulus coverage decreases about 22% per degree increase of CWT, analogous to an eye's iris when exposed to stronger light. They further inferred that the "iris" effect would produce a strong negative climate feedback. There have been intense debates about the validity of the "iris hypothesis" concerning the analysis approach and interpretation of the results [*Hartmann and Michelsen*, 2002a, 2002b, 2002c, hereafter HM2002; *Lindzen et al.*, 2002] as well as the assumptions of the radiative properties of high clouds [*Fu et al.*, 2002; *Lin et al.*, 2002; *Chambers et al.*, 2002; *Chou et al.*, 2002a, 2002b]. In particular, HM2002 argued that the definition of CWT may automatically produce a negative correlation of mean cloud fraction with CWT, provided that the variation of cloud fraction over the cold waters is much greater than that over the warm waters. They showed that the negative correlation of cirrus anvil fraction with CWT may arise from the large cloud variations in the subtropics driven by meteorological forcing associated with midlatitude storms. Constraining the averaging domain to lower latitudes away from the subtropics may avoid the definition problem of the CWT, but no reduction of anvil fraction relative to cumulus core fraction was found in the analysis of HM2002. *Del Genio and Kovari* [2002] analyzed the Tropical Rainfall Measuring Mission (TRMM) data and found that precipitation efficiency and cirrus detrainment efficiency both increase with increasing SST, with the former increasing faster than the latter. *Lin et al.* [2006] showed that the area coverage of tropical deep convective systems increases with SST along with their precipitation efficiency. *Rapp et al.* [2005] examined the ratio of deep convective cloud area to surface rainfall and found the ratio has no significant dependence on underlying SST, except for warm rain processes, where the cloud area to rainfall ratio decreases with SST, which may yield a positive feedback for reduced reflection of solar radiation. However, these studies were based on cloud information derived from TRMM data, which may underestimate thin cirrus clouds in the UT. A complete understanding of tropical high clouds and their radiative impacts requires more accurate and comprehensive cloud data sets.

[5] New satellite observations from the National Aeronautics and Space Administration (NASA)'s "A-train" satellite constellation [*Schoeberl and Talabac*, 2006] provide new information on global cloud variability. The A-train satellites are sun-synchronous, with equatorial crossing times around 1:30 am (descending orbits) and 1:30 pm (ascending orbits). The orbit tracks repeat every 16 days. In particular, the Atmospheric Infrared Sounder (AIRS) on the Aqua satellite [*Parkinson*, 2003; *Chahine et al.*, 2006] provides effective cloud fraction (CFR) and cloud top pressure (CTP), along with temperature and moisture profiles, information on trace gas species, and surface properties starting from September 2002. The Microwave Limb Sounder (MLS) on the Aura satellite [*Schoeberl et al.*, 2006; *Waters et al.*, 2006], for the first time, provides the upper tropospheric (UT) ice water content (IWC) profile at 215 hPa and above, starting from August 2004. The ice water path (IWP) can then be computed by the mass-weighted vertical integration of IWC from 215 hPa to the cloud top heights. The AIRS and MLS observations are only about 8 min apart [*Kahn et al.*, 2007], and there are about 5–6 AIRS measurements within each MLS field of view (FOV). CloudSat and CALIPSO are new members of the A-train (launched in June 2006) that measure cloud liquid and ice water content profiles throughout the troposphere [*Stephens et al.*, 2002]. However, the CloudSat/CALIPSO data are not used in this analysis.

[6] In this study, we present a new observational analysis of the UT cloud variations with SST. We analyze not only the UT cloud fraction (from AIRS), but also the IWC and IWP measurements (from MLS), which are critical to determine the cloud radiative forcing. The improved precision and coverage of these data sets compared to previous ones and especially the new vertically stratified IWC information enable new investigations of the cloud and SST relations. We use UT clouds to refer to the high-altitude clouds observed by AIRS and MLS without distinction between different cloud types or sources of origin. Separation of deep convective cores, anvil clouds and thin cirrus will be explored in future work. In contrast to a recent study by *Su et al.* [2006a], which analyzed the spatial correlation of MLS IWC/IWP with SST on monthly and annual timescales, this paper focuses on the temporal variation of UT CFR and IWC/IWP on a daily timescale, as in LCH2001. We are interested in the total cloud changes averaged over the entire tropics. *Zhang et al.* [1996] showed that the relationship of cloud radiative forcing and SST varies from basin to basin, and the cloud and SST relationship for more limited regions differs from that averaged over the entire tropics. These differences are caused by variability in the large-scale atmospheric circulation that complicates the SST influence on convection and associated cloud changes. Using an average over the entire tropics does include compensatory cloud changes due to large-scale circulations,

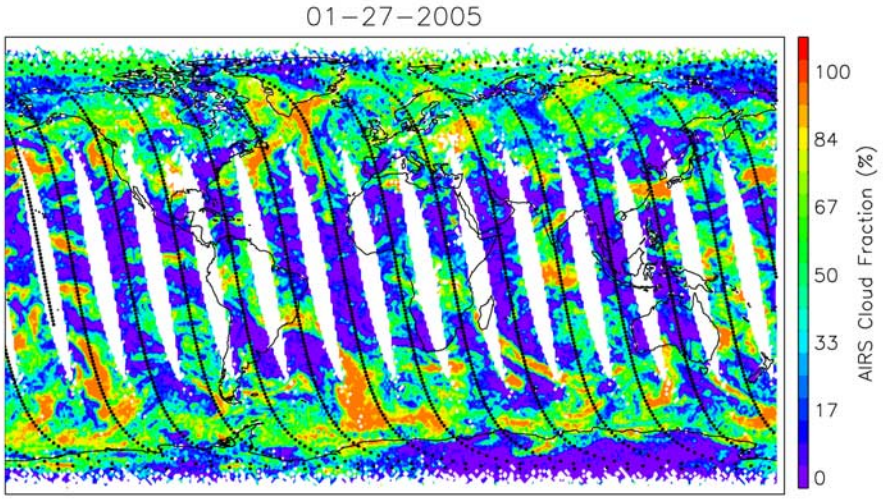

Figure 1. AIRS effective cloud fraction (color-shaded) on ascending orbit on 27 January 2005, along with MLS ascending orbit tracks (black dotted lines).

but avoids arbitrary boundary specifications and is more representative of changes in bulk cloud amount in response to the mean SST change. The observed relationships among these quantities can serve as useful references for global model simulations [e.g., *Su et al.*, 2006b].

[7] To facilitate the comparison with LCH2001, we use a similar analysis approach as used in their study: i.e., we examine the scatterplots of the UT CFR and IWC/IWP versus CWT and identify apparent relationships. We recognize the intrinsic problem of using the CWT definition as pointed out by HM2002. To deal with this problem, we have expanded the analysis into two parts. First, different tropical latitude belts are analyzed and compared. Second, the spatial patterns of UT CFR and IWC/IWP relations to CWT are examined so that the regional difference of cloud and SST relations are revealed. Moreover, the tropical-mean precipitation changes with CWT are investigated simultaneously and compared to that of the UT CFR and IWP. We also use precipitation to normalize CFR or IWP by dividing the mean CFR or IWP by the mean precipitation in an analogous procedure to LCH2001 which used deep cumulus core fraction to normalize cirrus anvil fraction. The relationships of the precipitation-normalized CFR and IWP with the CWT are analyzed, while the intricacies of the normalization procedure are addressed and the caveats of such a technique are noted.

[8] The structure of the paper is as follows. Section 2 describes the data sets used for the analyses. Section 3 presents the UT clouds and SST relationships based on the AIRS and MLS observations. The UT cloud radiative effect and its changes associated with the IWC/IWP changes are discussed in section 4. The conclusion and discussion are given in section 5.

2. Data

[9] We use AIRS Level 3 daily effective cloud fraction (CFR) and cloud top pressure (CTP) data on $1^\circ \times 1^\circ$ horizontal grids from 1 September 2002 to 30 September 2006 (version 4) [*Olsen*, 2005]. Both ascending (~1:30 pm local time) and descending (~1:30 am local time) orbits are included. Together they cover more than 90% of the globe, with each set of orbits alone covering about 80% of the globe (Figure 1). The AIRS CFR retrieval uses a radiance fitting procedure described by *Susskind et al.* [2003], with a horizontal resolution of ~15 km. To identify high-altitude clouds, we use the simultaneous AIRS Level 3 CTP measurement, which has a horizontal FOV of ~45 km in diameter, and has been validated against CloudSat, CALIPSO, and surface-based Atmospheric Radiation Measurement (ARM) observations [*Kahn et al.*, 2007a, 2007b]. Only grid boxes with CTP < 300 hPa are considered UT clouds. This value is chosen to match the MLS IWC measurement, which only goes down to 215 hPa. Early cross-comparison between the AIRS and MLS cloud measurements found that AIRS CTP tends to have a high pressure (i.e., low altitude) bias compared to that derived from the MLS IWC measurements [*Kahn et al.*, 2007a; *Wu et al.*, 2008]. We find that our results are not sensitive to the exact choices of CTP values between 450–200 hPa. Throughout the remainder of this work, we use CFR to denote the UT cloud fraction with CTP < 300 hPa. Note that the AIRS CFR represents a combined effect of cloud areal coverage and cloud emissivity. For thick clouds, the emissivity is close to 1. Their CFR is thus approximately fractional coverage. However, for thin clouds that are not opaque, the retrieved CFR is smaller than the actual cloud coverage. Preliminary analysis indicates that the difference between the AIRS retrieved CFR and the actual cloud coverage is about 0.2 (absolute difference) in the global average [*Kahn et al.*, 2007b]. Such caveats need to be considered when interpreting the results of the analysis.

[10] The Aura MLS Level 2 IWC measurements from 8 August 2004 to 30 September 2006 (version 1.5) are used. The IWC is retrieved from the cloud-induced radiance at 240 GHz [*Wu et al.*, 2006]. The v1.5 IWC is available at 215, 178, 147, 121, 100, 83 and 68 hPa, with a horizontal resolution of 200–300 km along-track and ~7 km cross-track, and a vertical resolution of 3–4 km [*Livesey et al.*, 2005; *Wu et al.*, 2006, 2008]. The Aura MLS IWC data

Table 1. Regression Slopes of Precipitation, CFR and IWP Versus the Cloud-Weighted SST for Different Tropical Areas[a]

	Precipitation	CFR	Precipitation-Normalized CFR	IWP	Precipitation-Normalized IWP
15°S–15°N	14%	13%	−2%	26%	15%
30°S–30°N	5%	6%	−1%	16%	10%
30°S–30°N, 130°E–170°W	7%	6%	0.1%	20%	10%

[a]Slopes are in the units of percentage change per K, relative to the multi-year means.

have been validated against in situ aircraft measurements and other satellite data [*Wu et al.*, 2008], and have been compared with model simulations and analyses [*Li et al.*, 2005]. The estimated IWC absolute accuracy is within a factor of 2 and there may be up to 50% low bias compared to CloudSat IWC (version 4) for single measurements, mostly for large IWC values due to instrument sensitivity [*Wu et al.*, 2008]. On averages over large spatial domain and over periods longer than a few days, the differences between MLS and CloudSat IWC are largely reduced [*Wu et al.*, 2008]. The spatial pattern of the MLS IWC resembles deep convective systems and associated anvil clouds [*Li et al.*, 2005; *Su et al.*, 2006a]. The Level 2 data are obtained along MLS orbit tracks. The gap between orbits is about 25° in the tropics (30°S–30°N) (Figure 1). The number of profiles each day is about 3500, with one-third of them within the tropics. Although the MLS daily data coverage is relatively sparse, the daily cloud occurrence frequency in the tropical average is close to the MLS monthly cloud occurrence frequency, suggesting that the tropical averages obtained from daily data are adequately representative of the entire tropics. We note that both AIRS and MLS measurements are only made up to twice per day for any given region and do not capture the full diurnal cycles of tropical clouds. Since the daily mean values are of interest here, the impact of diurnal variability is deferred to future study.

[11] We use the daily microwave SST product from the Advanced Microwave Scanning Radiometer–EOS (AMSR-E) on the Aqua satellite (version 2) with a horizontal resolution of 0.25° × 0.25°, processed at Remote Sensing Systems [*Donlon et al.*, 2002]. To reduce sampling errors, we average the AMSR-E SST to both AIRS and MLS data grids when performing correlation analyses. The through-cloud capabilities of microwave radiometers reduce the influence of clouds on the SST retrieval, and the daily coverage of the AMSR-E SST is an improvement from the weekly SST product from the National Centers for Environmental Prediction (NCEP) analysis, which was used in LCH2001.

[12] We use the daily TRMM precipitation data (3B42) [*Huffman et al.*, 2001] at a horizontal resolution of 0.25° × 0.25°. Averaging onto the AIRS and MLS data grids is performed for coincident sampling, as for the AMSR-E SST.

3. UT Clouds and SST Relations

[13] The daily mean UT cloud amount is defined as $\bar{A} = [\sum_n \cos\theta_n \cdot A_n]/\sum_n \cos\theta_n$, where A is either CFR, IWC or IWP, θ is the latitude, and n includes only oceanic measurements. For tropical mean SST, we use the cloud-weighted SST definition as in LCH2001, i.e., $\mathrm{CWT} = [\sum_n CFR_n \cos\theta_n \cdot SST_n]/\sum_n CFR_n \cos\theta_n$. This reflects the importance of under-cloud SST as the forcing of cloud changes. We present the scatterplots of UT clouds versus the CWT for averages over 15°S–15°N. The results for averages over 30°S to 30°N and the area used in LCH2001 are summarized in Table 1 for comparison purpose. Besides the tropical mean cloud CFR, IWC and IWP relationship with the cloud-weighted SST, the spatial correlation of UT clouds with the cloud-weighted SST, and composite zonal means of UT clouds, precipitation and SST variations are also analyzed.

3.1. AIRS CFR-SST Relation

[14] Figure 2a shows the AIRS tropical-mean UT cloud fraction ($\overline{CFR}$) scattered against the cloud-weighted SST for 15°S–15°N during the period of 1 September 2002 to 30 September 2006. Each dot corresponds to a daily average. All daily $\overline{CFR}$ occurs over the CWT greater than 300 K, indicating the close connection of AIRS observed UT clouds to tropical deep convection [e.g., *Graham and Barnett*, 1987; *Waliser et al.*, 1993; *Su et al.*, 2006a]. The daily $\overline{CFR}$ is quite scattered with respect to the CWT, but a positive slope is discernible, about 1.6 CFR% K^{-1} (∼13% K^{-1} relative to the 4-year mean CFR of 12%). The correlation coefficient is about 0.2, rejecting the null hypothesis of zero correlation at the 95% significance level based on the Student's t-test. If we extend the area to 30°S–30°N, the regression slope reduces to 0.5 CFR% K^{-1} (∼6% K^{-1} relative to the 4-year mean CFR), with a correlation coefficient of 0.16 (Table 1). If we perform the averaging over the western Pacific from 130°E to 170°W (30°S–30°N) as in LCH2001, the slope of CFR versus SST is 0.8 CFR% K^{-1}, or 6% K^{-1} relative to its 4-year mean, with a correlation coefficient of 0.12 (Table 1). The smaller regression slope of CFR versus the CWT for areas including the subtropics indicates that the weaker SST influence away from the deep convective regions. However, the correlation coefficients between the mean cloud fraction and the CWT are generally weak in all regions examined, with the values even smaller than those in HM2002 using the original data sets as LCH2001. Furthermore, the sign is reversed here.

[15] The positive correlation of AIRS CFR with the CWT is different from the negative correlation of anvil cloud coverage with the CWT as shown in LCH2001. This may be because the AIRS CFR includes deep convective towers, anvil clouds and even thin cirrus while LCH2001 separated anvil clouds from cumulus turrets. Second, the emissivity factor in the AIRS CFR may cause biases in the CFR and CWT relation. Moreover, our data set covers different periods from LCH2001 and interannual variability may play a role in the different relations of UT cloud fraction versus SST. Using the first two years and last two years of daily CFR regressed with the corresponding CWT gives a positive slope of 1.1 and 1.9 CFR% K^{-1} (9% K^{-1} and 16% K^{-1}

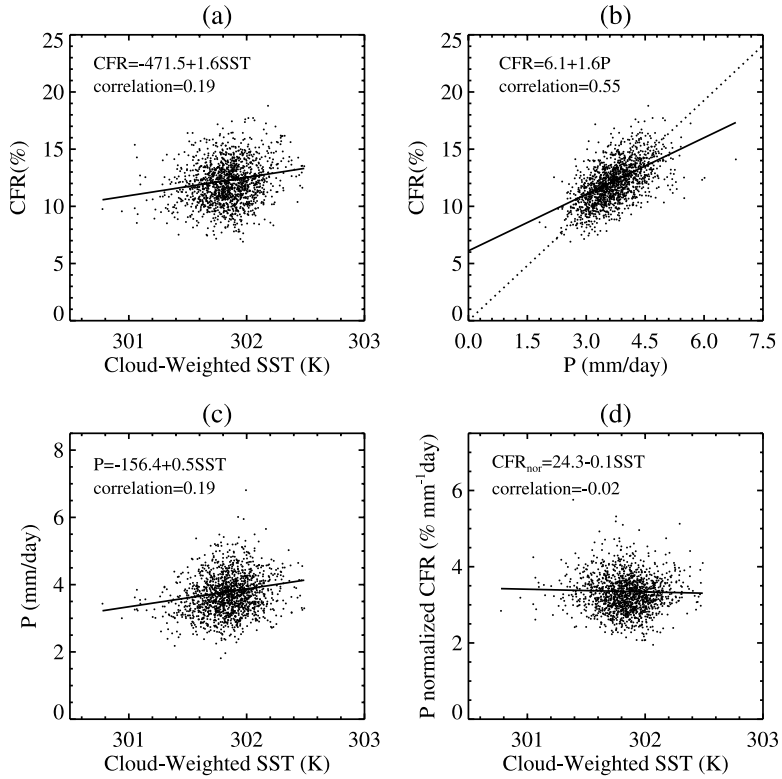

Figure 2. Scatterplots of (a) the tropical-averaged (15°S–15°N) CFR (CTP < 300 hPa) versus cloud-weighted SST, (b) the tropical-averaged CFR versus the tropical-averaged precipitation, (c) the tropical-averaged precipitation versus the cloud-weighted SST, and (d) the precipitation-normalized CFR (in % mm^{-1} day) versus the cloud-weighted SST. Each point is a daily value from 1 September 2002 to 30 September 2006. The solid lines are the least squares linear fits to the data, with the corresponding equations shown. The dotted line in Figure 2b marks the regression line constrained to go through zero (see text for details).

relatively), respectively. Despite the difference in the magnitudes for different years, the AIRS CFR appears to increase with the CWT.

[16] To examine the spatial distribution of the CFR relation to the CWT, we follow the analysis techniques used in HM2002 to regress the time series of CFR at each 1° × 1° grid onto the time series of CWT (averaged over 30°S–30°N). The regressions are performed using both the original unfiltered data and high-passed data, in which a 91-day running mean is removed to filter out the low-frequency variability. We find the spatial patterns of regression coefficients are similar using the unfiltered or high-passed data as in HM2002. Figure 3 shows the regression coefficients of CFR on the CWT which has been high-pass filtered and divided by its standard deviation. Consistent with HM2002, the regression coefficients of CFR on the CWT exhibit spatial differences in deep tropics and subtropics; but to a much less extent than that in HM2002. The regression coefficients are positive in climatologically convective regions and negative in non-convective regions, with minima in the subtropical North Pacific and the southern Indian Ocean. As HM2002 pointed out, negative regression of CFR with CWT tends to occur over cold waters. However, we note that the magnitudes of regression coefficients in Figure 3 are mostly within ±0.05 per standard deviation change of the CWT, much smaller than the values in

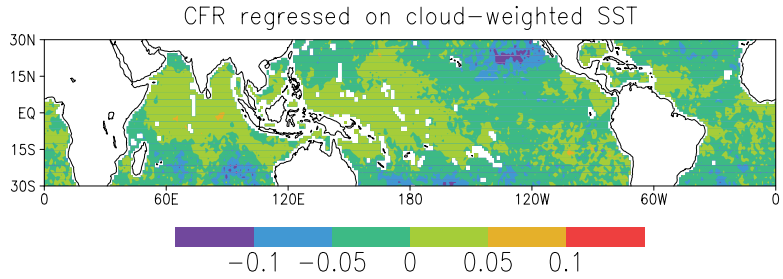

Figure 3. Regression coefficients of AIRS CFR onto the high-pass cloud-weighted SST. The cloud-weighted SST is divided by its standard deviation.

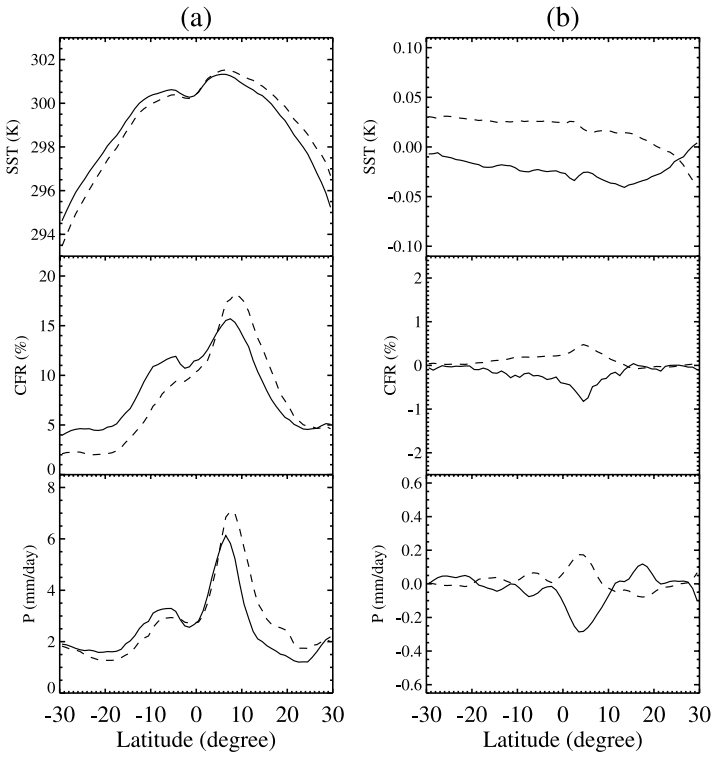

Figure 4. Zonal averages of SST, CFR and precipitation for days when the cloud-weighted SST is less than average (solid lines) and for days when the cloud-weighted SST is greater than average (dashed lines), (a) unfiltered data and (b) high-passed data.

HM2002 for cirrus anvil fraction (based on $T_b < 260$ K) regressed on the CWT. This may be due to the different data sets used. The UT cloud fraction derived from AIRS data includes deep convective cores and thin cirrus generated from convective detrainment and in situ formation [e.g., *Boehm and Verlinde*, 2000]. They appear to be less sensitive to the underlying SST change than the anvil fraction based on $T_b < 260$ K by HM2002.

[17] LCH2001 hypothesized that increasing precipitation efficiency with increasing surface temperature may reduce the cirrus outflow. We analyzed the TRMM precipitation data set and examined its variation with SST and CFR. Figure 2b shows the scatterplot of the $\overline{CFR}$ versus the mean precipitation ($\overline{P}$) for 15°S–15°N. The correlation coefficient between $\overline{CFR}$ and $\bar{P}$ is 0.55, statistically significant above the 95% level. When $\bar{P}$ is scattered against the CWT, a positive correlation of 0.2 is found (Figure 2c). The $\bar{P}$ increases with the CWT at a rate of 0.5 mm day^{-1} K^{-1}, about 14% K^{-1} relative to its 4-year mean. When we define a precipitation-normalized CFR by simply dividing $\overline{CFR}$ by $\bar{P}$ and scatter the ratio of cloud fraction to precipitation against the CWT, we find the precipitation-normalized cloud fraction appears to be insensitive to SST changes, with a slightly negative slope of −0.1 CFR% mm^{-1} day K^{-1} (Figure 2d), corresponding to −2% K^{-1} relative to the 4-year mean. The correlation coefficient between the precipitation-normalized cloud fraction and the CWT is only −0.02, suggesting virtually no linear correlation.

[18] However, a caveat needs to be pointed out regarding this normalization procedure, which is analogous to the normalization of cirrus anvil fraction by deep convective core fraction used by LCH2001. As shown in Figure 2b, tropical-mean cloud fraction is not simply proportional to the tropical-mean precipitation, since the linear regression line has a non-zero intercept. Thus simply dividing cloud fraction by precipitation would result in a term inversely proportional to the mean precipitation in addition to the regression slope of cloud fraction to precipitation, and only the latter is the quantity of relevance to the detrainment of cirrus clouds per unit convection. Hence, although the normalization is appealing, simply dividing the cloud fraction by precipitation does not provide a good solution to isolate the cirrus detrainment change from the cumulus convection change itself. Given the non-proportionality between cloud fraction and precipitation, we are inclined to be cautious about inferring cirrus detrainment change using this normalization procedure.

[19] For the entire tropics within 30°S–30°N, the precipitation-normalized CFR also shows a slightly negative regression slope with the CWT, about −1% K^{-1} (Table 1), but the correlation coefficient is close to zero. For the region analyzed in LCH2001, the slope of the precipitation-normalized CFR versus SST is only 0.1% K^{-1}, an almost flat regression line. Considering that the AIRS CFR convolves emissivity and areal coverage, the actual cirrus areal coverage is higher than the CFR, especially for thin cirrus [*Kahn et al.*, 2007b]. This may yield a somewhat stronger negative slope in Figure 2d if warmer SST is associated with thicker UT clouds.

[20] Figure 4 further illustrates the relations among SST, cloud fraction and precipitation in terms of zonal averages. It shows the composite zonal mean SST, CFR and precip-

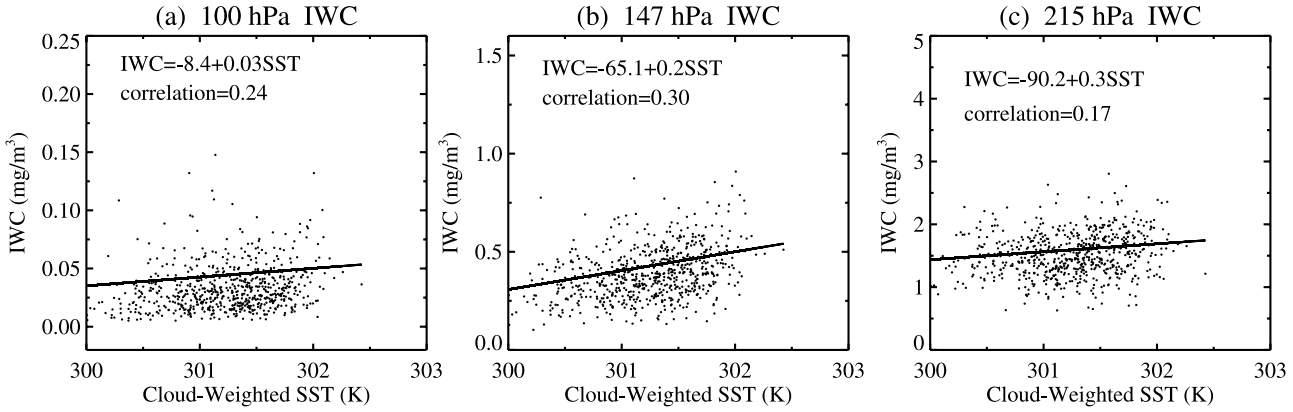

Figure 5. Scatterplots of tropical-averaged (15°S–15°N) IWC versus the cloud-weighted SST at three pressure levels, (a) 100 hPa, (b) 147 hPa, and (c) 215 hPa. Each point is a daily value from 8 August 2004 to 30 September 2006. The solid lines are the least squares linear fits to the data, with the corresponding equations shown.

itation for days when CWT was lower than the 4-year average (solid lines, the "lower SST days") and vice versa (dashed lines, the "higher SST days") using both unfiltered (Figure 4a) and high-passed (91-day running mean removed, Figure 4b) data. Although this composite procedure was similar to HM2002, the results we obtain bear different characteristics from HM2002 (their Figure 5), mainly because different data sets are analyzed here, which may be associated with different cloud systems. In HM2002, the anti-correlation of CWT with anvil cloud fraction primarily resulted from the cloud fraction variations in latitudes greater than 15°. The equatorial anvil cloud fraction changes were smaller than those in the subtropics. In our composites (Figure 4), the CWT seems in phase with the northern hemispheric SST and out of phase with the southern hemisphere SST, arising from the seasonal shifts of SST patterns. Since the cloud fraction in the northern hemisphere is larger on average than that in the southern hemisphere, the CWT variation is dominated by the northern hemispheric SST. Noticeable differences in cloud fraction between the "lower SST days" and the "higher SST days" are found through all tropical latitudes, which are positively correlated with each hemispheric zonal SST changes. Similarly, zonal precipitation changes follow the zonal SST changes. Figure 4b shows the zonal-mean SST, CFR and precipitation variations when seasonal cycles are removed. Again, we find CFR and precipitation changes positively correlate with SST changes for most tropical latitudes. Large changes of CFR and precipitation are within 10°S–10°N. Outside 10°S–10°N, the changes of CFR and precipitation are quite small.

[21] In summary, the tropical-mean UT cloud fraction has a weakly positive correlation with the underlying SST. We do not observe a negative correlation of the UT CFR with the CWT as by LCH2001. Comparing to the precipitation increase with the CWT, the UT cloud fraction increases at a similar rate. No distinct correlation is found between the CWT and the ratio of the UT CFR to the precipitation.

[22] On the other hand, CFR is only one measure of UT cloud amount. Cloud optical depth, which is dependent on IWC and cloud height, is a more radiatively relevant cloud quantity. The changes of IWC with SST can alter the net radiative forcing of the UT clouds in addition to that caused by the cloud fraction changes. Therefore we have analyzed the IWC measurements from MLS to better quantify the UT cloud variations with SST.

3.2. MLS IWC-SST Relation

[23] Figure 5 shows the daily tropical-mean MLS IWC scattered against the CWT for 15°S–15°N during the period from 8 August 2004 to 30 September 2006. The definition of $\overline{IWC}$ is similar to $\overline{CFR}$. For each day, the CWT is computed using the AMSR-E SST weighted by the AIRS CFR, both sampled onto the MLS IWC measurement location. Three vertical levels of IWC are shown in Figure 5, 100 hPa (~16 km), 147 hPa (~13.5 km) and 215 hPa (~11 km). All exhibit an increase of $\overline{IWC}$ with increasing CWT, albeit with a large scatter. The rates of the $\overline{IWC}$ increase with the CWT are 0.3 mg m^{-3} K^{-1} at 215 hPa, 0.2 mg m^{-3} K^{-1} at 147 hPa and 0.03 mg m^{-3} K^{-1} at 100 hPa. The percentage changes relative to the 2-year mean at each level are approximately 15% K^{-1} at 215 hPa, 34% K^{-1} at 147 hPa, and 60% K^{-1} at 100 hPa. The correlation coefficients between the IWC and the CWT are about 0.2 at 215 hPa, 0.3 at 147 hPa and 0.2 at 100 hPa, all statistically significant above the 95% level.

[24] Figure 6 shows the scatterplot of the vertically integrated IWC, i.e., IWP, versus the CWT, and the scatterplots of IWP versus precipitation and the precipitation-normalized IWP versus the CWT. The rate of the increase of the $\overline{IWP}$ with the CWT is 1.4 g m^{-2} K^{-1}, about 26% K^{-1} relative to the 2-year mean IWP. The correlation coefficient between $\overline{IWP}$ and the CWT is about 0.3. The tropical-mean precipitation $\bar{P}$ is positively correlated with $\overline{IWP}$ with a correlation coefficient of 0.6. However, we note that $\overline{IWP}$ and $\bar{P}$ are not strictly proportional, indicated by the two different slopes for the least squares fitted line and the line constrained to go through zero (Figure 6b). Thus the relation of the precipitation-normalized IWP with SST (Figure 6c) does not completely remove the precipitation dependence on SST, similar to the precipitation-normalized CFR shown in Figure 2d. Despite the fact that the term inversely proportionally to precipitation would yield a negative tendency for the precipitation-normalized IWP relation with SST, the precipitation-normalized IWP exhib-

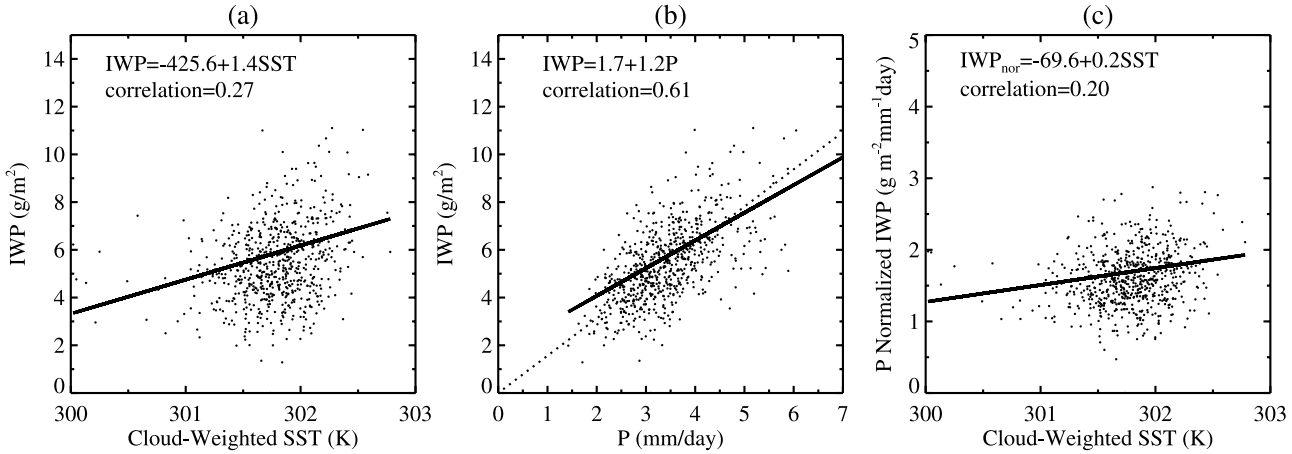

Figure 6. Scatterplots of (a) the tropical-averaged (15°S–15°N) IWP (integrated from 215 hPa) versus the cloud-weighted SST, (b) the tropical-averaged IWP versus the tropical-averaged precipitation, and (c) the precipitation-normalized IWP (in g m^{-2} mm^{-1} day) versus the cloud-weighted SST. Each point is a daily value from 8 August 2004 to 30 September 2006. The solid lines are the least squares linear fits to the data, with the corresponding equations shown. The dotted line in Figure 6b marks the regression line constrained to go through zero (see text for details).

its a positive slope with the CWT, at the rate about 15% K^{-1}, with a correlation coefficient of 0.2. Similar results are found for 30°S–30°N and the region used in LCH2001 (Table 1). The increase of $\overline{IWP}$ with the CWT occurs at a greater rate than that of precipitation for all three areas analyzed.

[25] The composite zonal averages of SST, IWP and precipitation are shown in Figure 7 for the days when the CWT is higher (dashed lines) or lower (solid lines) than the

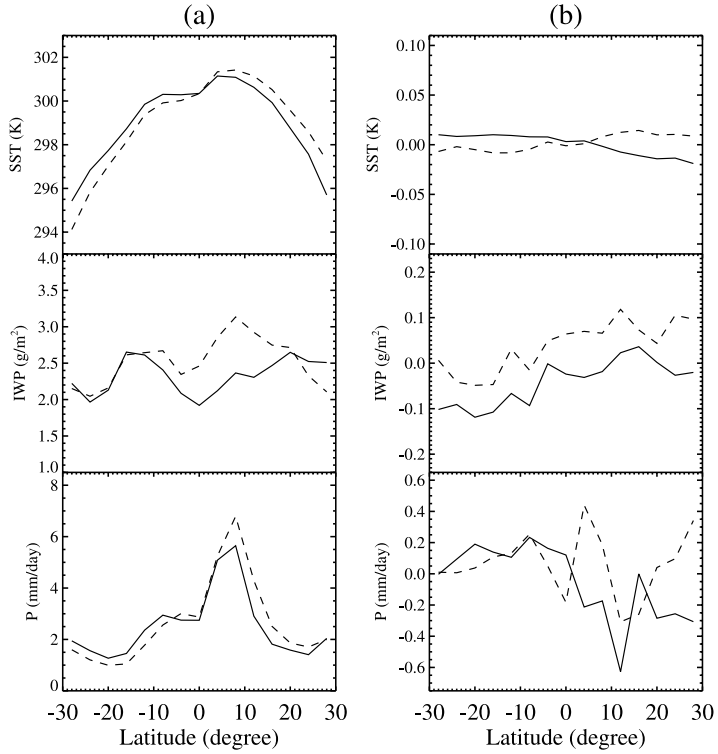

Figure 7. Zonal averages of SST, IWP and precipitation for days when the cloud-weighted SST is less than average (solid lines) and for days when the cloud-weighted SST is greater than average (dashed lines), (a) unfiltered data; (b) high-passed data. The SST and precipitation are interpolated to the MLS IWC measurement location and 2-years of data from August 2004 to September 2006 are used here.

2-year mean. Compared to the zonal means in Figure 4 based on the 4-year $1^\circ \times 1^\circ$ gridded data, the zonal averages constructed from the 2-year data on the MLS tracks appear noisier. The high-passed (91-day running mean removed) zonal-mean SST (Figure 7b, top panel) shows little difference ($\sim$0.02 K) between the ''higher SST days'' and the ''lower SST days'' for the two years. Nevertheless, both the unfiltered and high-passed data show that the higher CWT is associated with larger IWP for most of tropical latitudes. The precipitation tracks the SST latitudinal variation quite well, even though the high-passed precipitation is very noisy. Similar to Figure 4b, it is not obvious that the subtropical cloud variations are greater than that in the deep tropics, different from the results shown in HM2002.

4. Exploring the Radiative Effect of UT Clouds

[26] The motivation to examine the UT cloud fraction and IWC changes with SST resides in the importance of the radiative forcing of these clouds to the Earth-atmosphere climate system. It is useful to estimate how much the cloud radiative effect may change given the rate of UT cloud changes with SST. However, a limitation of our data sets is the lack of cloud profiles below 215 hPa. Thus an accurate quantification of the total cloud radiative forcing is not possible with only the data sets used in this study. Nevertheless, we carry out some calculations to obtain a qualitative estimate of the radiative effect of the UT clouds and the sensitivity of the cloud radiative effect to UT cloud changes. Our calculations are focused on the tropical-mean cloud forcings. These calculations are considered to be idealized but they help to shed light on understanding the cloud feedback problem.

[27] The radiative transfer model we use is the Fu-Liou radiation model. It uses the delta-four-stream approximation for solar flux calculations [*Liou et al.*, 1988] and delta-two-stream approximation for infrared flux calculations [*Fu et al.*, 1997]. The incorporation of non-grey gaseous absorption in multiple-scattering atmospheres is based on the correlated *k*-distribution method developed by *Fu and Liou* [1992]. The solar and infrared spectra are divided into 6 and 12 bands, respectively, according to the location of absorption bands. Parameterization of the single-scattering properties for ice cloud follows the procedure developed by *Fu and Liou* [1993]. The spectral extinction coefficient, the single-scattering albedo, and the asymmetry factor are parameterized in terms of the IWC and the effective ice crystal size (D_e). For D_e, instead of using the mono-distribution as in the standard Fu-Liou code, we adopt the empirical formula for ice particle size distribution developed by *McFarquhar and Heymsfield* [1997] (the MH distribution) as used in the MLS IWC forward model, where D_e is computed as a function of MLS measured IWC and temperature. This treatment of ice particle size is consistent with the MLS IWC retrieval and is considered to be an improvement over other more arbitrary assumptions of ice particle size.

[28] We perform the radiation calculations for two cases. In one case, we treat all MLS observed UT clouds as 'single-layer' clouds, with no clouds underneath (the ''single-layer'' case). This treatment has been a common practice in isolation of the radiative effect of certain types of clouds [e.g., *Fu and Liou*, 1993; *Hartmann et al.*, 2001; *Fu et al.*, 2002]. Another case takes into account the influence of lower clouds by using the tropical climatological values for both the low and middle-altitude clouds from the International Satellite Cloud Climatology Project (ISCCP) [*Rossow and Schiffer*, 1991] below the AIRS and MLS observed UT clouds, with random overlapping in the vertical (the ''multi-layer'' case). The UT cloud radiative effect (CRE) is thus the difference of LW and SW fluxes at the top of atmosphere (TOA) with and without the observed UT clouds while other conditions (surface, atmospheric profiles and low and middle-altitude clouds) are held the same.

[29] Because of the non-linearity of cloud radiation calculations, it is necessary to compute the radiative fluxes using instantaneous UT cloud profiles along orbit tracks, rather than using averaged profiles over a certain area or period. The monthly tropical-mean CRE is then constructed by averaging all individual CREs, totaling about 35000 calculations per month within the tropics (30°S–30°N). For both clear-sky and all-sky radiative flux calculations, the standard tropical atmospheric profile is used instead of the observed atmospheric profiles such as those from AIRS. Using a uniform atmospheric profile isolates the cloud forcing due to cloud properties alone rather than the convoluted effects from clouds and associated temperature and water vapor changes [*Soden et al.*, 2004].

[30] We consider that each MLS measurement footprint has fractional cloud coverage η, determined by the AIRS UT cloud fraction interpolated on the MLS FOV. Since the MLS measurements represent the averaged IWC over the MLS FOV, the actual overcast IWC value is IWC/η. We test the sensitivity of CRE to the estimate of η by augmenting AIRS CFR by 0.2 (the ''+0.2 CFR run'') or assuming that the UT cloud coverage for each MLS IWC FOV is 100% and the AIRS CFR equals the cloud emissivity (the ''overcast run'').

[31] Using January 2005 as an example, Table 2 lists the calculated monthly tropical-mean UT cloud forcing for different radiation model runs. In the ''single layer'' case, assuming η = AIRS CFR, the net UT cloud CRE is about 2.7 W m^{-2} (warming) in the tropical average, with LW CRE being 4.7 W m^{-2} and SW CRE being -2.0 W m^{-2}. Increasing η by 0.2 would increase the LW and SW CREs by 0.3 and 0.03 W m^{-2} in magnitude, respectively, resulting in 3.0 W m^{-2} warming in the tropical average. The ''overcast'' run yields a significantly larger LW warming effect. The tropical-averaged net CRE becomes 17.6 W m^{-2}, with 21.4 W m^{-2} LW CRE and -3.8 W m^{-2} SW CRE.

[32] In the ''multi-layer'' case, we use the low and middle cloud climatology taken from *Dessler et al.* [1996], which were based on the ISCCP data for February–March 1984 to 1988, averaged over 0°–10°S. The low clouds are specified from 855 hPa to 760 hPa, with a visible optical depth of 20 and a fraction of 19%. The middle-altitude clouds are specified from 525 hPa to 462 hPa, with a visible optical depth of 10 and a fraction of 16%. Both have an emissivity of 1. The cloud effective radii are 11 μm for middle clouds and 10 μm for low clouds [*Dessler et al.*, 1996]. The UT cloud fractional

Table 2. Tropical-Mean (30°S–30°N) LW, SW and Net CRE (in W m^{-2}) in January 2005 for the Radiative Model Runs

	LW CRE	SW CRE	Net CRE
Single-layer case standard run	4.74	−2.00	2.74
Single-layer case +0.2 CFR run	5.05	−2.03	3.02
Single-layer case overcast run	21.39	−3.82	17.57
Multi-layer case standard run	4.28	−1.44	2.84

coverage η is based on the AIRS CFR interpolated onto the MLS IWC measurement location. Under the random overlapping assumption, we obtain a tropical mean OLR of 268 W m^{-2}, and a tropical reflectivity of 0.3. Compared to the Earth Radiation Budget Experiment (ERBE) tropical climatology [*Barkstrom*, 1984], the OLR is overestimated by 5% and the reflectivity is overestimated by about 30%. The Clouds and the Earth's Radiant Energy System (CERES) tropical climatology gives a slightly higher OLR and reflectivity than ERBE and the errors of our estimates relative to CERES are still close to 30% for SW fluxes. However, because the UT cloud forcing is of interest, we focus our attention on the differences of TOA LW and SW fluxes with and without UT clouds. In the "multilayer" case, the LW CRE of the UT cloud is smaller than the "single-layer" case by 0.4 W m^{-2} in the tropical average as the low and middle clouds reduce the terrestrial emission reaching the upper levels. The SW CRE also decreases to −1.5 W m^{-2}, resulting in a net CRE of 2.8 W m^{-2}, close to the "single-layer" case (Table 2). Varying the low and middle cloud optical properties moderately does not change the magnitude of UT CRE significantly.

[33] Our estimates of the net UT cloud forcing are consistent with previous results of high cloud forcing calculated from models or obtained from observations. *Hartmann et al.* [1992] regressed the ERBE radiative flux data on the ISCCP cloud data to investigate the radiation effect of each cloud type. They found that high thin cloud (optical depth less than 9.38, cloud top <440 hPa) produced a net warming of 2.3 W m^{-2} in DJF in the global-average. *Chen et al.* [2000] calculated the radiative effect of each ISCCP cloud type in a radiative transfer model and showed that cirrus cloud (optical depth < 3.6, cloud top < 440 hPa) has a net warming of 1.3 W m^{-2} at TOA in the global average. For "overcast" high clouds, the model calculations by *Hartmann et al.* [2001] and *Fu et al.* [2002] suggested that high clouds with cloud top pressure less than 300 hPa and optical depth less than 4 have a net warming effect around 20 W m^{-2}. When multiplied by their fractional coverage, the net high cloud forcing is on the order of a few W m^{-2}. As 99% of the MLS observed ice clouds have optical depth less than 4, they fall into the category of high thin clouds or cirrus by the ISCCP definition. Our calculated UT CREs are within the range of previous theoretical or observational estimates, especially for tropical-means. Qualitatively, these UT clouds alone would produce a net warming at TOA.

[34] Since the UT IWC tends to increase with SST more than does the cloud fraction, we conduct a set of sensitivity runs to investigate the change of CRE due to the changes of IWC. We successively increase the IWC values at each height uniformly over the tropics by 25% to 250%, while keeping cloud fraction unchanged. For simplicity, the "single-layer" approach is used. Based on the previous calculations (Table 2), the results obtained from the "single-layer" case is applicable to the "multilayer" case, in terms of the sign and approximate magnitude of UT CRE. Figure 8 shows that the tropical-mean net warming reaches its maximum when IWC is increased by 25%–50% from the current value. When IWP is increased by 50%, The net warming is 0.05 W m^{-2} more than the standard run, with LW and SW effects both increasing by approximately 0.7 W m^{-2} (slightly more for LW). Supposing the rate of IWC increase with SST is about 26% K^{-1} as shown in Figure 6a and Table 1, the change of net CRE with SST is about 0.02 W m^{-1} K^{-1}, while the separate changes of LW and SW CRE are larger. When IWC is increased more than 50%, the increase in SW cooling outweighs LW

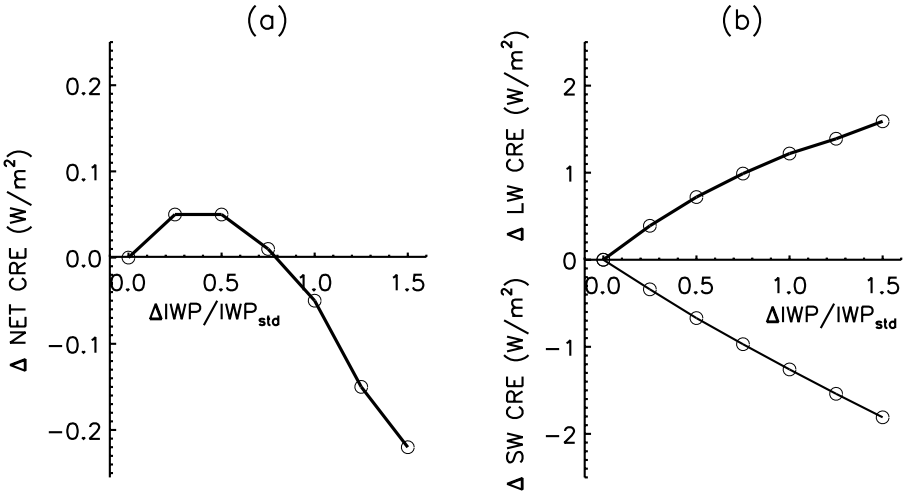

Figure 8. The changes of tropical-mean CREs (a) net, (b) LW and SW (in W m^{-2}) when the tropical-mean IWP is increased successively. The *x* axis is the percentage increase of IWP relative to the presently observed value by MLS. All results are based on the January 2005 UT cloud profiles, assuming no low and middle clouds underneath.

warming, causing the net CRE to decrease from its maximum value. When IWC is increased by 75%, the net CRE returns to approximately the same value as the standard run, although the changes in the LW and SW effects are both about 1.0 W m^{-2} in the tropical average. A further increase of IWC yields net warming smaller than the standard run, although it is unlikely the polarity of the net CRE would reverse sign given reasonable IWC changes for hypothetical SST changes up to a few degrees. These UT clouds would provide a persistent warming effect even when their IWC is more than doubled. Note that these sensitivity runs also provide an estimate of UT cloud forcing errors when the bias in MLS IWC measurements is considered. The doubled IWC run gives an upper bound of cloud forcing uncertainty (<0.05 W m^{-2}) due to the low bias in MLS IWC single measurements. If all MLS IWC measurements were 50% lower than the actual IWC, further increase of UT IWC would tend to reduce the net warming and correspond to a negative cloud feedback. However, since the tropical-mean MLS IWC is not significantly lower than that of CloudSat, our estimate of tropical-mean UT CRE is useful in a reasonable range.

5. Conclusion and Discussion

[35] Two aspects of tropical upper tropospheric cloud variations with SST are analyzed using new cloud observations from AIRS and MLS. One aspect is UT cloud area fraction (CFR) and the other is ice water content (IWC), which is directly linked to cloud optical thickness. Averages of cloud quantities and precipitation over tropical oceans are scattered against the cloud-weighted SST (CWT) and their relationships with the CWT are identified. Daily tropical-mean UT cloud fraction from AIRS tends to increase with the CWT, at a comparable rate to the tropical-mean precipitation increase with the CWT, about 13% K^{-1} for 15°S–15°N and 6% K^{-1} for 30°S–30°N. Measures of UT cloud ice, IWC and IWP, are found to increase with the CWT at a rate ~26% K^{-1} for 15°S–15°N and ~16% K^{-1} for 30°S–30°N, faster than does the tropical-mean precipitation. The reduced rates of increase with the CWT when more subtropical areas are included in averaging may suggest the influence of midlatitude storms [*HM2002*]. Examination of the zonal-averages of SST, CFR, IWP and precipitation shows that the positive correlations of CFR and IWP with the CWT occur universally over the deep tropics within 10–15 degrees from the equator. Further away from the equator into the subtropics, dynamical effects not related to SST may contaminate the CFR and IWP relations with the CWT. However, we do not find greater CFR or IWP changes in the subtropics than in the deep tropics as by HM2002. Instead, the AIRS CFR and MLS IWP show relatively large changes within the deep tropics.

[36] We also adopt a procedure as by LCH2001 which normalizes CFR or IWP by precipitation and regress the ratio with the CWT. Although the intent of normalizing cloud statistics by a measure related to convective mass flux is appealing [*LCH2001*], we show that such a normalization procedure that assumes proportionality appears to face inherent problems. For the data considered here, proportionality does not hold between precipitation and CFR or IWP. While the normalization procedure thus does not appear to be a reliable means of taking out the effects of large-scale circulations and SST gradients, and we do not recommend it for inference regarding climate change, we nonetheless examine the results of this procedure, and do not find a significant negative relationship with CWT. However, the observed variations of UT CFR, IWC, IWP and precipitation with the CWT provide useful reference values for evaluation of cloud simulations in climate models.

[37] The radiative effect of the UT clouds observed by AIRS and MLS is estimated using the Fu-Liou radiative transfer model. We emphasize the qualitative aspect of the radiation calculations due to uncertainties associated with missing low and middle level clouds, the estimate of cloud fraction and other factors. We find that UT clouds have a dominant infrared-warming effect owing to their small visible optical depth, consistent with previous studies. Increasing the UT IWC by 50% would increase the net cloud forcing by about 0.05 W m^{-2}, corresponding to a small positive feedback and a sensitivity to SST around 0.02 W m^{-2} K^{-1}. However, the small change in net CRE is associated with relatively large changes in LW and SW fluxes separately, which can have a non-negligible effect on atmospheric heating rate and surface energy budget. Further increases of IWC would reduce the magnitude of net warming due to the nonlinearity in the net CRE with IWC. However, for any reasonable increase of tropical mean SST (within a few degrees), the net radiative forcing of these UT clouds remains positive (warming). Measurement uncertainties in UT CFR and IWC greatly affect the magnitude of cloud forcing but the qualitative change of cloud radiative effects holds for a reasonable range.

[38] We note that our analysis focuses on the upper-most clouds in the troposphere. We do not find a negative correlation of the UT cloud fraction with the underlying SST. The variations of the UT clouds with SST are consistent with increases in tropical deep convection with SST, with the caveat that this is in part associated with changes in SST gradients for the variability observed here. The implication that stronger convection produces thicker cirriform clouds when local SST increases qualitatively agrees with RC1991, although the radiative effect of UT clouds derived here is different from the cloud forcing by RC1991, which included the deep convective clouds and anvils in the whole tropospheric column. With the emerging new tropospheric cloud profiles from CloudSat/CALIPSO, we are hopeful that a better understanding of tropical cloud variability and a more accurate quantification of cloud radiative impact can be attained.

[39] **Acknowledgments.** We thank MLS and AIRS colleagues for data support. Discussions with A. Dessler, Q. Fu, B. Lin, R. S. Lindzen, and R. Rondanelli were helpful. This work was carried out at the Jet Propulsion Laboratory, California Institute of Technology, under contract with NASA. JDN is supported by National Science Foundation Grant ATM-0645200 and NOAA Grant NA05OAR4311134. We thank three anonymous reviewers for helpful comments and suggestions.

References

Barkstrom, B. R. (1984), The Earth Radiation Budget Experiment (ERBE), *Bull. Am. Meteorol. Soc.*, *65*, 1170–1185.

Betts, A. K. (1990), Greenhouse warming and the tropical water budget, *Bull. Am. Meteorol. Soc.*, *71*, 1464–1465.

Boehm, M. T., and J. Verlinde (2000), Stratospheric influence on upper tropospheric tropical cirrus, *Geophys. Res. Lett.*, *27*(19), 3209–3212.
Bony, S., J.-L. Dufresne, H. LeTreut, J.-J. Morcrette, and C. Senior (2004), On dynamic and thermodynamic components of cloud changes, *Clim. Dyn.*, *22*, 71–86.
Cess, R. D., et al. (1990), Intercomparison and interpretation of climate feedback processes in 19 atmospheric GCMs, *J. Geophys. Res.*, *95*(D10), 16,601–16,615.
Cess, R. D., et al. (1996), Cloud feedback in atmospheric general circulation models: An update, *J. Geophys. Res.*, *101*(D8), 12,791–12,794.
Chahine, T. M., T. S. Pagano, H. H. Aumann, R. Atlas, C. Barnet, et al. (2006), AIRS: Improving weather forecasting and providing new data on greenhouse gases, *Bull. Am. Meteorol. Soc.*, *87*(7), 911–926.
Chambers, L., B. Lin, and D. Young (2002), New CERES data examined for evidence of tropical iris feedback, *J. Clim.*, *15*, 3719–3726.
Chen, T., W. B. Rossow, and Y. Zhang (2000), Radiative effects of cloud-type variations, *J. Clim.*, *13*, 264–286.
Chou, M.-D., R. S. Lindzen, and A. Y. Hou (2002a), Reply to: "Tropical cirrus and water vapor: An effective Earth infrared iris feedback?", *Atmos. Chem. Phys.*, *2*, 99–101.
Chou, M.-D., R. S. Lindzen, and A. Y. Hou (2002b), Comments on "The Iris hypothesis: A negative or positive cloud feedback?", *J. Clim.*, *15*, 2713–2715.
Del Genio, A. D., and W. Kovari (2002), Climatic properties of tropical precipitating convection under varying environmental conditions, *J. Clim.*, *15*, 2597–2615.
Dessler, A. E., K. Minschwaner, E. M. Weinstock, E. J. Hintsa, J. G. Anderson, and J. M. Russell III (1996), The effects of tropical cirrus clouds on the abundance of lower stratospheric ozone, *J. Atmos. Chem.*, *23*, 209–220.
Donlon, C. J., P. Minnett, C. Gentemann, T. J. Nightingale, I. J. Barton, B. Ward, and J. Murray (2002), Towards improved validation of satellite sea surface skin temperature measurements for climate research, *J. Clim.*, *15*(4), 353–369.
Fu, Q., and K. N. Liou (1992), On the correlated k-distribution method for radiative transfer in nonhomogeneous atmospheres, *J. Atmos. Sci.*, *49*, 2139–2156.
Fu, Q., and K. N. Liou (1993), Parameterization of the radiative properties of cirrus clouds, *J. Atmos. Sci.*, *50*, 2008–2025.
Fu, R., A. D. Del Genio, W. B. Rossow, and W. T. Liu (1992), Cirrus-cloud thermostat for tropical sea surface temperatures tested using satellite data, *Nature*, *358*, 394–397.
Fu, Q., K. N. Liou, M. Cribb, T. P. Charlock, and A. Grossman (1997), Multiple scattering in thermal infrared radiative transfer, *J. Atmos. Sci.*, *54*, 2799–2812.
Fu, Q., M. Baker, and D. L. Hartmann (2002), Tropical cirrus and water vapor: An effective earth infrared iris feedback?, *Atmos. Chem. Phys.*, *2*, 1–7.
Graham, N. E., and T. P. Barnett (1987), Sea surface temperature, surface wind divergence, and convection over tropical oceans, *Science*, *238*, 657–659.
Hartmann, D. L., and K. Larson (2002), An important constraint on tropical cloud-climate feedback, *Geophys. Res. Lett.*, *29*(20), 1951, doi:10.1029/2002GL015835.
Hartmann, D. L., and M. L. Michelsen (1993), Large-scale effects on regulation of tropical sea surface temperature, *J. Clim.*, *6*, 2049–2062.
Hartmann, D. L., and M. L. Michelsen (2002a), No evidence for iris, *Bull. Am. Meteorol. Soc.*, *83*, 249–254.
Hartmann, D. L., and M. L. Michelsen (2002b), Reply to the comments on "No evidence for iris", *Bull. Am. Meteorol. Soc.*, *83*, 1349–1352.
Hartmann, D. L., and M. L. Michelsen (2002c), A two-box model of cloud-weighted sea surface temperature: The semiautomatic negative correlation with mean cloud fraction, *Bull. Am. Meteorol. Soc.*, *83*, 1352.
Hartmann, D. L., M. E. Ockert-Bell, and M. L. Michelsen (1992), The effect of cloud type on Earth's energy balance: Global analysis, *J. Clim.*, *5*, 1281–1304.
Hartmann, D. L., L. Moy, and Q. Fu (2001), Tropical convection and the energy balance at the top of the atmosphere, *J. Clim.*, *15*, 4495–4511.
Huffman, G. J., R. F. Adler, M. Morrissey, D. T. Bolvin, S. Curtis, R. Joyce, B. McGavock, and J. Susskind (2001), Global precipitation at one-degree daily resolution from multi-satellite observations, *J. Hydrometeorol.*, *2*(1), 36–50.
Kahn, B. H., et al. (2007a), Cloud type comparisons of AIRS, CloudSat, and CALIPSO cloud height and amount, *Atmos. Chem. Phys. Discuss.*, *7*, 13,915–13,958.
Kahn, B. H., A. Eldering, A. J. Braverman, E. J. Fetzer, J. H. Jiang, E. Fishbein, and D. L. Wu (2007b), Towards the characterization of upper tropospheric clouds using atmospheric infrared sounder and microwave limb sounder observations, *J. Geophys. Res.*, *112*, D05202, doi:10.1029/2006JD007336.
Lau, K.-M., H.-T. Wu, and S. Bony (1997), The role of large-scale atmospheric circulation in the relationship between tropical convection and sea surface temperature, *J. Clim.*, *10*, 381–392.
Li, J.-L., et al. (2005), Comparisons of EOS MLS cloud ice measurements with ECMWF analyses and GCM simulations: Initial results, *Geophys. Res. Lett.*, *32*, L18710, doi:10.1029/2005GL023788.
Lin, B., B. Wielicki, L. Chambers, Y. Hu, and K.-M. Xu (2002), The iris hypothesis: A negative or positive cloud feedback?, *J. Clim.*, *15*, 3–7.
Lin, B., B. A. Wielicki, P. Minnis, L. Chambers, K.-M. Xu, Y. Hu, and A. Fan (2006), The effect of environmental conditions on tropical convective systems observed from the TRMM satellite, *J. Clim.*, *19*, 5745–5761.
Lindzen, R. S. (1990), Some coolness concerning global warming, *Bull. Am. Meteorol. Soc.*, *71*, 288–299.
Lindzen, R. S., and S. Nigam (1987), On the role of sea surface temperature gradients in forcing low level winds and convergence in the tropics, *J. Atmos. Sci.*, *44*, 2418–2436.
Lindzen, R. S., M.-D. Chou, and A. Y. Hou (2001), Does the Earth have an adaptive infrared iris, *Bull. Am. Meteorol. Soc*, *82*, 417–432.
Lindzen, R. S., M.-D. Chou, and A. Y. Hou (2002), Comments on "No evidence for iris", *Bull. Am. Meteorol. Soc.*, *83*, 1345–1348.
Liou, K. N., Q. Fu, and T. P. Ackerman (1988), A simple formulation of the delta-four-stream approximation for radiative transfer parameterizations, *J. Atmos. Sci.*, *45*, 1940–1947.
Livesey, N. J., et al. (2005), EOS MLS Version V1.5 Level 2 data quality and description document, available at http://mls.jpl.nasa.gov.
Massie, S., A. Gettelman, W. Randel, and D. Baumgardner (2002), Distribution of tropical cirrus in relation to convection, *J. Geophys. Res.*, *107*(D21), 4591, doi:10.1029/2001JD001293.
McFarquhar, G. M., and A. J. Heymsfield (1997), Parameterization of tropical cirrus ice crystal size distributions and implications radiative transfer: Results from CEPEX, *J. Atmos. Sci.*, *54*, 2187–2200.
Olsen, E. T., (ed.) (2005), AIRS/AMSU/HSB Version 4.0 Data Release User Guide, JPL Document, available at http://disc.gsfc.nasa.gov/AIRS/documentation/v4_docs/V4_Data_Release_UG.pdf, NASA Goddard Space Flight Center, Maryland.
Parkinson, C. L. (2003), Aqua: An Earth-observing satellite mission to examine water and other climate variables, *IEEE Trans. Geosci. Remote Sens.*, *41*(2), 173–183.
Pierrehumbert, R. T. (1995), Thermostats, radiator fins, and the local runaway greenhouse, *J. Atmos. Sci.*, *52*, 1784–1806.
Ramanathan, V., and W. Collins (1991), Thermodynamics regulation of ocean warming by cirrus clouds deduced from observations of the 1987 El Nino, *Nature*, *351*, 27–32.
Rapp, A., C. Kummerow, W. Berg, and B. Griffith (2005), An evaluation of the proposed mechanism of the adaptive infrared iris hypothesis using TRMM VIRS and PR measurements, *J. Clim.*, *18*, 4185–4194.
Rossow, W. B., and R. A. Schiffer (1991), ISCCP cloud data products, *Bull. Am. Meteorol. Soc.*, *72*, 2–20.
Schoeberl, M. R., and S. Talabac (2006), The Sensor Web: A future technique for science return, in *Observing Systems for Atmospheric Composition*, edited by G. Visconti et al., pp. 203–206, Springer, New York.
Schoeberl, F., et al. (2006), Overview of the EOS Aura Mission, *IEEE Trans. Geosci. Remote Sens.*, *44*, 1066–1074.
Soden, B. J., and R. Fu (1995), A satellite analysis of deep convection, upper-tropospheric humidity, and the greenhouse effect, *J. Clim.*, *8*, 2333–2351.
Soden, J. B., A. J. Broccoli, and R. S. Hemler (2004), On the use of cloud forcing to estimate cloud feedback, *J. Clim.*, *17*, 3661–3665.
Stephens, G. L. (2005), Cloud feedbacks in the climate system: A critical review, *J. Clim.*, *18*, 237–273.
Stephens, G. L., et al. (2002), The CloudSat mission and the A-Train: A new dimension of space-based observations of clouds and precipitation, *Bull. Am. Meteorol. Soc.*, *83*(12), 1771–1790.
Su, H., W. G. Read, J. H. Jiang, J. W. Waters, D. L. Wu, and E. J. Fetzer (2006a), Enhanced positive water vapor feedback associated with tropical deep convection: New evidence from Aura MLS, *Geophys. Res. Lett.*, *33*, L05709, doi:10.1029/2005GL025505.
Su, H., D. E. Waliser, J. H. Jiang, J.-L. Li, W. G. Read, J. W. Waters, and A. M. Tompkins (2006b), Relationships of upper tropospheric water vapor, clouds and SST: MLS observations, ECMWF analyses and GCM simulations, *Geophys. Res. Lett.*, *33*, L22802, doi:10.1029/2006GL027582.
Sun, D. Z., and R. S. Lindzen (1993), Distribution of tropical tropospheric water vapor, *J. Atmos. Sci.*, *50*, 1644–1660.
Sun, D. Z., and Z. Liu (1996), Dynamic ocean-atmosphere coupling: A thermostat for the tropics, *Science*, *272*, 1148–1150.
Susskind, J., C. D. Barnet, and J. M. Blaisdell (2003), Retrieval of atmospheric and surface parameters from AIRS/AMSU/HSB data in the presence of clouds, *IEEE Trans. Geosci. Remote Sens.*, *41*, 390–409.

Tompkins, A. M., and G. C. Craig (1999), Sensitivity of tropical convection to sea surface temperature in the absence of large-scale flow, *J. Clim.*, *12*(2), 462–476.

Udelhofen, P. M., and D. L. Hartmann (1995), Influence of tropical cloud systems on the relative humidity in the upper troposphere, *J. Geophys. Res.*, *100*(D4), 7423–7440.

Waliser, E. D., N. E. Graham, and C. Gautier (1993), Comparison of the highly reflective cloud and outgoing longwave radiation datasets for use in estimating tropical deep convection, *J. Clim.*, *6*, 331–353.

Wallace, J. M. (1992), Effect of deep convection on the regulation of tropical sea surface temperature, *Nature*, *357*, 230–231.

Waters, J. W., et al. (2006), The Earth Observing System Microwave Limb Sounder (EOS MLS) on the Aura satellite, *IEEE Trans. Geosci. Remote Sens.*, *44*, 1075–1092.

Wu, D. L., J. H. Jiang, and C. P. Davis (2006), EOS MLS cloud ice measurements and cloudy-sky radiative transfer model, *IEEE Trans. Geosci. Remote Sens.*, *44*, 1156–1165.

Wu, D. L., J. H. Jiang, W. G. Read, R. T. Austin, C. P. Davis, A. Lambert, G. L. Stephens, D. G. Vane, and J. W. Waters (2008), Validation of the Aura MLS cloud Ice Water Content (IWC) measurements, *J. Geophys. Res.*, *113*, D15S10, doi:10.1029/2007JD008931.

Zhang, M. H., R. D. Cess, and S. C. Xie (1996), Relationship between cloud radiative forcing and sea surface temperature over the entire tropical oceans, *J. Clim.*, *9*, 1374–1384.

D. Feldman and Y. L. Yung, Division of Geological and Planetary Sciences, California Institute of Technology, MC 170-25, 1200 E. California Blvd., Pasadena, CA 91125, USA.

Y. Gu and J. D. Neelin, Department of Atmospheric and Oceanic Sciences, University of California, Los Angeles, 405 Hilgard Ave., Los Angeles, CA 90095-1565, USA.

J. H. Jiang, B. H. Kahn, N. J. Livesey, W. G. Read, M. L. Santee, H. Su, and J. W. Waters, Jet Propulsion Laboratory, California Institute of Technology, M/S 183-701, 4800 Oak Grove Drive, Pasadena, CA 91109-8099, USA. (hui.su@jpl.nasa.gov)